AD-A095 450 NAVAL RESEARCH LAB WASHINGTON DC F/G 20/6
EVIDENCE FOR SELF-FOCUSING OR FILAMENTATION FROM X-RAY, 3/2 OME--ETC(U)
FEB 81 M J HERBST, J A STAMPER, R R WHITLOCK
UNCLASSIFIED NRL-MR-4434 NL

1 OF 1
AD A 095450

END
DATE FILMED
3-81
DTIC

NRL Memorandum Report 4434

Evidence for Self-Focusing or Filamentation from X-ray, 3/2 ω_0, and 2 ω_0 Emission

M. J. HERBST, J. A. STAMPER, R. R. WHITLOCK, R. H. LEHMBERG, AND B. H. RIPIN

Laser Plasma Branch
Plasma Physics Division

February 5, 1981

NAVAL RESEARCH LABORATORY
Washington, D.C.

(14) NRL-MR-4434

SECURITY CLASSIFICATION OF THIS PAGE (When Data Entered)

REPORT DOCUMENTATION PAGE

READ INSTRUCTIONS BEFORE COMPLETING FORM

1. REPORT NUMBER: NRL Memorandum Report 4434

2. GOVT ACCESSION NO.: (9) Memorandum Rept.

3. RECIPIENT'S CATALOG NUMBER:

4. TITLE (and Subtitle): (6) EVIDENCE FOR SELF-FOCUSING OR FILAMENTATION FROM X-RAY, $3/2\,\omega_0$, AND $2\,\omega_0$ EMISSION.

5. TYPE OF REPORT & PERIOD COVERED: Interim report on a continuing NRL problem.

6. PERFORMING ORG. REPORT NUMBER:

7. AUTHOR(s): (10) M. J. Herbst, J. A. Stamper, R. R. Whitlock, R. H. Lehmberg and B. H. Ripin

8. CONTRACT OR GRANT NUMBER(s): (11) 5 Feb 81

9. PERFORMING ORGANIZATION NAME AND ADDRESS: Naval Research Laboratory, Washington, D.C. 20375

10. PROGRAM ELEMENT, PROJECT, TASK AREA & WORK UNIT NUMBERS: 47-0859-A-1

11. CONTROLLING OFFICE NAME AND ADDRESS: Department of Energy, Washington, D.C. 20545

12. REPORT DATE: February 5, 1981

13. NUMBER OF PAGES: 15

14. MONITORING AGENCY NAME & ADDRESS (if different from Controlling Office):

15. SECURITY CLASS. (of this report): UNCLASSIFIED

15a. DECLASSIFICATION/DOWNGRADING SCHEDULE:

16. DISTRIBUTION STATEMENT (of this Report)

Approved for public release; distribution unlimited.

17. DISTRIBUTION STATEMENT (of the abstract entered in Block 20, if different from Report)

18. SUPPLEMENTARY NOTES

19. KEY WORDS (Continue on reverse side if necessary and identify by block number)

Filamentation
Self-focusing
X-ray imaging
Harmonic emission

20. ABSTRACT (Continue on reverse side if necessary and identify by block number)

With long pulse, moderate intensity ($\simeq 10^{13}$ W/cm^2) Nd-laser irradiation of flat targets, time-integrated images of $3/2\,\omega_0$ and $2\,\omega_0$ emission reveal filaments along the laser axis. Combined with fine-scale structure found in time-integrated images of x-ray emission, these filaments suggest self-focusing of hot spots in the incident beam.

DD FORM 1 JAN 73 1473 EDITION OF 1 NOV 65 IS OBSOLETE
S/N 0102-LF-014-6601

SECURITY CLASSIFICATION OF THIS PAGE (When Data Entered)

25 195

EVIDENCE FOR SELF-FOCUSING OR FILAMENTATION FROM X-RAY, $3/2\,\omega_0$, AND $2\,\omega_0$ EMISSION

A crucial requirement for laser fusion is that the pressure driving the pellet implosion be sufficiently uniform that no shell breakup occurs before maximum compression.[1] With 1.06 μm laser wavelength, driver energy is directly deposited no closer to solid density than at the critical density surface where $n_e = n_c = 10^{21}$ cm^{-3}. If this absorption region is sufficiently far from the solid density ablation surface, pressure non-uniformities present at the absorption surface may be smoothed out by thermal transport between absorption and ablation regions.[1] Even in the presence of this smoothing, however, it is desirable to have the pressure profile at the absorption region be as uniform as possible. As this pressure depends upon incident irradiance, pressure uniformity requires uniformity of illumination. At least two mechanisms exist for destroying illumination uniformity at the absorption region: 1) illumination geometry or imperfect laser optics, and 2) plasma effects such as self-focusing or filamentation.[2,3] The latter are more important in the larger plasmas envisaged for laser fusion reactors than in the smaller plasmas of present experiments.

To simulate the interaction of a long pulse-length laser with the large spherical plasmas anticipated in laser fusion reactors, 100-200J, 4-nsec pulses from the Pharos II 1.054 μm Nd laser are focused to large spot diameters (0.5 - 1.0 mm) on flat targets of polystyrene (CH) or aluminum. Structure observed in time-integrated images of x-ray emission suggest fine-scale laser intensity modulation, a signature of self-focusing. More direct evidence for variation of the irradiance on this small spatial scale is obtained from time-integrated images of $3/2\omega_0$ and $2\omega_0$ emission.

Manuscript submitted November 5, 1980.

Except for the laser pulse duration and the speed of the incident focusing lens (f/6 in this case), the experimental arrangement is as described previously.[4] Visible emission is collected at 90° to the target normal by an f/2 lens and imaged through narrow-band filters and a polarization discriminator (Wollaston prism) with a factor of five magnification onto Polaroid positive-negative film (for $2\omega_o$) or Kodak type I-N spectroscopic plates (for $3/2\ \omega_o$). An x-ray pinhole camera with a 17.8 μm beryllium filter ($h\nu \gtrsim 1$ keV) views the rear of the laser-irradiated targets. Images are obtained with magnifications near three on either Kodak No-Screen film (for CH targets) or 3490 film (for Al targets).

Large-scale nonuniformities observed in x-ray images provide evidence for correlation between x-ray emission intensity and incident laser intensity. Linear fringes (100-200μm spacing) are observed regularly both in x-ray images (Fig. 1A) and in isointensity profiles of the incident laser focal distribution (Fig. 1B). Vidicon scans of the focal profiles imply that the incident intensity modulation associated with these patterns is about 2:1.

On a smaller spatial scale, modulation is observed in the x-ray images that is not observed in the incident beam. The finest scale of laser focal structure observed at the 2:1 modulation level is 50-80 μm; while even finer scale structure may exist, it must have significantly lower modulation level. X-ray images, however, do show much finer scale structure, as shown in Fig. 1C. These spots are observed in images of both CH and Al targets, though the number of observed spots is much greater with the Al. Reducing pinhole size to the limit allowed by signal-to-noise considerations allows an upper limit of 20 μm to be placed on the diameter d at the source of these observed spots when average incident irradiance

(A) X-RAY IMAGE (B) LASER FOCUS (C) X-RAY IMAGE

Fig. 1 — A) Rear-side x-ray image for 12.5μm Al foil target at $I_o \simeq 5.3 \times 10^{12}$ W/cm^2; B) isointensity contour from same shot as (A); (C) Rear side x-ray image for 7 μm Al foil target at $I_o \simeq 6.1 \times 10^{12}$ W/cm^2.

I_o exceeds 5×10^{12} W/cm^2. Evidence that d varies with I_o is found at $I_o \lesssim 2.5 \times 10^{12}$ W/cm^2, where measured d's are comparable in size to the 50-80 μm structure in the incident beam.

As the rear side x-ray camera views x-ray transmission through the target from the front side, an experimental check is made to insure that the spots represent variations in front side emission rather than variations in target thickness (and, therefore, transmission). A camera viewing the front side of the target does see pinhole-resolution limited spots which correlate with those observed by the rear camera; for Al targets the spots are observed only when the frontal camera is equipped with an Al filter to reduce Al line emission relative to continuum emission from the blowoff plasma.

Since the spots do reflect variations in x-ray emission and x-ray emission is seen, at least for the large-scale nonuniformities, to be correlated with incident irradiance variations, one might infer that the spots reflect laser intensity modulation on a fine spatial scale. If the absence of these small-scale structures in the incident focal profile is not just due to limitations of our laser beam diagnostic, this suggests self-focusing of hot spots in the laser beam.

More direct evidence for fine-scale modulation of the irradiance is found at $n_c/4$ and n_c by side-on imaging of 3/2 ω_o and 2 ω_o emission, respectively. Near threshold for detection of 3/2 ω_o radiation (average intensity $I_o \simeq 1.0 \times 10^{13}$ W/cm^2), filamentary structures are seen with either emitted light polarization, as shown in Fig. 2A. These filaments have transverse dimensions as small as 6 μm and lengths greater than 200μm. As I_o is increased by a factor of 2, threshold for detection of 3/2 ω_o

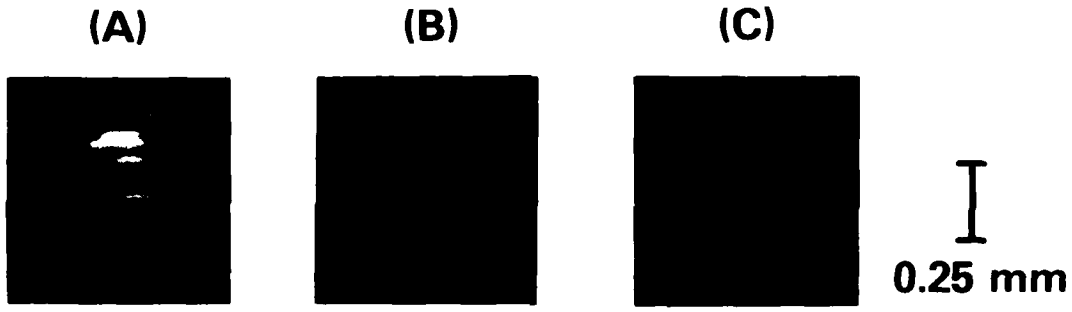

Fig. 2 — 3/2 ω_o images for CH targets: (A) central region of 1mm laser spot on 40 μm foil at $I_o \simeq 1.1 \times 10^{13}$ W/cm^2; (B) 42.7 μm thick, 500 μm diameter disk at $I_o \simeq 2.0 \times 10^{13}$ W/cm^2, with emitted light polarization corresponding to incident laser; and (C) same shot as (B), but with orthogonal polarization. Laser is incident from left in all images.

emission from the entire $n_c/4$ surface is exceeded. Two lobes of emission are observed in emitted light with polarization corresponding to the incident laser (Fig. 2B); curiously, a much different image is observed in the orthogonal polarization (Fig. 2C). Filamentary structures are also found in time-integrated images of $2\omega_o$ emission with $I_o \gtrsim 5 \times 10^{12}$ W/cm^2, as seen in Fig. 3. The large region of uniform exposure is visible continuum, as verified by substitution of filters which exclude $2\omega_o$; only the filaments along the laser axis are unique to $2\omega_o$. Again, transverse dimensions $\lesssim 10\mu$m are observed, with lengths up to 125μm, and emission is observed only with polarization corresponding to the incident laser.

At least three mechanisms can cause spurious lengthening of the observed $3/2\ \omega_o$ and $2\ \omega_o$ images in the direction along the laser axis, leading to the filamentary appearance. Target motion[4] during the period of emission might stretch images; this effect is easily eliminated by using thicker targets which do not move. Even with a stationary target, the $n_c/4$ or n_c density surface may move during the evolution of the blowoff plasma; this effect has not been eliminated and may be important. Finally, refraction of the emitted light by the blowoff plasma can have an effect. Rays emitted from a point into different angles are bent differently, appear to originate from different sources, and lead to lengthening of the observed image.

Simple ray tracing calculations of the refracted ray paths are performed for point sources at $n_c/4$ (for $3/2\ \omega_o$) and n_c (for $2\omega_o$) in a plane-stratified plasma with an exponential density profile. For a density gradient scale length $L_n = (n_e^{-1}\ dn_e/dx)^{-1}$ at $n_c/4$ of 100-125μm, the observed length of $3/2\ \omega_o$ structures could be explained solely

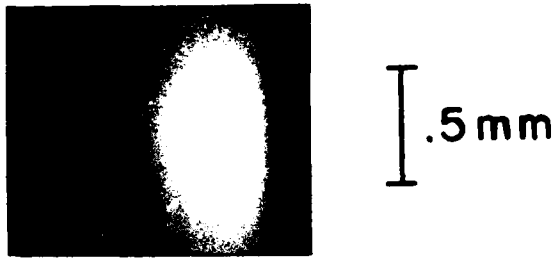

Fig. 3 — $2\omega_o$ image for 7 μm CH target at $I_o \simeq 1.1 \times 10^{13}$ W/cm^2. Laser is incident from left, and dark vertical edge at right is target surface. General exposure due to emitted continuum is seen in addition to filaments of emitted $2\omega_o$.

by refraction. The double-lobed pattern observed in Fig. 2B may also be a signature of refraction; for a certain range of L_n one region of emission may appear as two since two isolated sets of rays, one near 90^o and one propagating up toward critical density, are bent into the f/2 collection cone. Refraction does not, however, explain the difference observed at higher I_o between images with the two polarizations (Figs. 2B vs. 2C). One possible explanation is that two production mechanisms are operative in different regions of the blowoff plasma and each is responsible for one of the observed polarizations.

The length of the $2\omega_o$ images could also be explained by refraction, though this requires a large scalelength ($\gtrsim$200 μm) at n_c. Additionally, at the highest intensities used ($I_o \simeq 2 \times 10^{13}$ W/cm^2), faint images of parts of a $2\omega_o$ surface are seen on the downstream (laser) side of the filaments. As this surface has much smaller axial extent than the filaments, these images suggest that refraction is not the sole cause of filament length. The fact that the filaments are observed on the upstream side of the surface suggests that if the filament length is not due to time integration, the density within the channel must be lower than outside. A higher density channel would perturb the critical surface toward the underdense plasma, and filaments would be seen downstream from the surface.

Regardless of the cause of the observed length of the visible images, the transverse modulation must be considered. Since the conversion efficiency of light from ω_o to harmonics is a function of density gradient scalelength, regions of greater harmonic emission may either have higher I_o or different L_n. The efficiency of conversion from ω_o to $3/2\ \omega_o$ is a monotonically increasing function of L_n.[6,7,8] As one would expect

localized structures to have shorter scale lengths than the rest of the blowoff, the 3/2 ω_o production would be reduced, if anything, for a given incident intensity in the observed channels. We may then estimate a lower bound for the intensity modulation at $n_c/4$ by assuming that L_n in the filaments and in the remainder of the blowoff are equal. As the 3/2 ω_o from the blowoff becomes detectable at twice the intensity at which the filaments are seen, one infers a lower bound of 2:1 for the level of intensity modulation. This lower bound is the same as the 2:1 intensity modulation level present in the incident beam, though that structure has larger spatial scale.

A similar analysis of the $2\omega_o$ images would give an intensity modulation at n_c of 4:1, with parts of a complete surface just being seen at 4 times the intensity at which the filaments are seen. Theoretically, the dependence of $2\omega_o$ generation on L_n is non-monotonic, however, maximizing at density gradient scale lengths of several wavelengths.[9,10] It is possible, therefore, to have enhanced 2 ω_o generation due to shorter L_n; in that case, it is not clear whether the inferred intensity modulation is an overestimate or underestimate. Certainly a 4:1 modulation would represent a definite increase over the modulation present on the incident beam.

Finally, we estimate the expected propagation distance required for a significant increase of intensity modulation due to self focusing or filamentation. For the collisionally dominated regime encountered in these experiments, filamentation arises primarily from the electron heating and concomitant decrease of plasma density in the more intense parts of the beam.[11] A perturbation treatment of this effect, which balances inverse Bremsstrahlung heating and classical transverse thermal conduction in a

uniform plasma,[12] yields the spatial growth rate $\alpha = (\alpha_o^2 - \pi^2\lambda^2/\varepsilon\lambda_\perp^4)^{\frac{1}{2}}$, where $\alpha_o = (n_e/n_c)\left[I\nu/(1 + Z^{-1})\varepsilon^{3/2} c\, TK\right]^{\frac{1}{2}}$ would be the growth rate without diffraction. In these expressions, $\lambda_\perp$ is the wavelength of the transverse perturbation, I is the incident hot spot intensity, ν is the collision frequency, Z is the average ionization state, $\varepsilon = 1 - n_e/n_c$ is the plasma dielectric constant, T is the local temperature, and K is the thermal conductivity. A CH plasma (Z = 3.5) of density $n_c/4$ and T = 400 eV thus gives an e-folding length $\alpha^{-1} \simeq 340$ μm for $\lambda_\perp = 50$μm and $I = 10^{13}$ W/cm^2 (the intensity at which the x-ray spots seem to shrink). At the highest intensity used, approximately 4×10^{13} W/cm^2 in the hot regions, this reduces to $\alpha^{-1} \simeq 160$ μm. An Al plasma (Z = 13) under these conditions gives $\alpha^{-1} \simeq 95$ μm for 10^{13} W/cm^2 and 45 μm for 4×10^{13} W/cm^2. This increase of filamentation growth with ionization state is in qualitative agreement with our x-ray observations. Given our large underdense plasmas, one does expect an increase in intensity modulation over that present in the incident beam.

The experimental results are consistent, then, with self-focusing of hot spots in the incident laser beam. This would account for the observed localization of x-ray emission in small spots, as well as the transverse modulation of $3/2\omega_o$ and $2\omega_o$ emission. The observations are strong circumstantial evidence, though, and not concrete proof. The fine scale-variations at the absorption region which would result from this self-focusing might not have serious consequences for laser fusion. As the distance between absorption and ablation surfaces is likely to be large compared to the spatial scale of the pressure nonuniformity, this may easily wash out due to lateral conduction in the region between the two. For this reason, the larger-scale

variations in pressure corresponding to the 100-200 μm structure in the x-ray images and incident beam, may be a much greater threat to successful uniform compression of laser fusion pellets.

The authors wish to acknowledge useful conversation with Drs. S.E. Bodner and S.P. Obenschain and with Mr. J. Grun. The expert technical assistance of M. Fink, N. Nocerino, L. Seymour and E. Turbyfill is greatly appreciated. This work was supported by the U.S. Department of Energy and Office of Naval Research.

REFERENCES

1. J. Nuckolls, et al. Nature, 239, 139 (1972).

2. P. Kaw, et al. Phys. Fluids 16, 1522 (1973).

3. B.I. Cohen and C.E. Max, Phys. Fluids, 22, 1115 (1979).

4. B.H. Ripin, et al., Phys. Fluids, 23, 1012 (1980).

5. N.K. Winsor and D.A. Tidman, Phys. Rev. Lett. 31, 1044 (1973) and D.G. Colombant, et al., Phys. Fluids 18, 1687 (1975).

6. C.S. Liu and M.N. Rosenbluth, Phys. Fluids 19, 967 (1976).

7. A.I. Avrov, et al., Sov. Phys. JETP 45, 507 (1977).

8. B. Lasinski, private communication.

9. W.L. Kruer and K.G. Estabrook, in Laser Interaction and Related Plasma Phenomena, Vol. 4B, ed. by H.J. Schwarz and H. Hora, (Plenum, New York, 1977), p. 709.

10. N.S. Erokhin, et al. Nuc. Fusion 14, 333 (1974) and Sov. Phys. JETP 29, 101 (1969).

11. M.S. Sodha, et al., Prog. Opt. 13, 169 (1976).

12. V.K. Tripathi and L.A. Pitale, J. Appl. Phys. 48, 3288 (1977).

DISTRIBUTION LIST

USDOE (50 copies)
P.O. Box 62
Oak Ridge, TN 37830

National Technical Information Service (24 copies)
U.S. Department of Commerce
5285 Port Royal Road
Springfield, VA 22161

NRL, Code 2628 (35 copies)

NRL, Code 4730 (100 copies)

NRL, Code 4700 (25 copies)

USDOE (6 copies)
Office of Inertial Fusion
Washington, D.C.
Attn: Dr. G. Canavan
Dr. R. Schriever
Dr. S. Kahalas
Dr. T. Godlove
Dr. K. Gilbert

Lawrence Livermore Laboratory
P.O. Box 808
Livermore, CA 94551
Attn: Dr. D. Attwood, L481
Dr. W. Kruer, L545
Dr. B. Lasinski
Dr. C. Max, L545
Dr. A. Glass
Dr. L. Coleman
Dr. J. Nuckolls
Dr. W. Mead
Dr. N. Ceglio
Dr. R. Kidder

INTERNAL DISTRIBUTION

Code 4790 Dr. D. Colombant
Dr. W. Manheimer

Department of Physics and Astronomy
University of Maryland
College Park, MD 20740
Attn: Dr. H. Griem

Los Alamos Scientific Laboratory
Los Alamos, NM 87545
Attn: Dr. R. Godwin
Dr. D. Giovanielli
Dr. J. Kindel, Dr. D. Forslund

University of Rochester
Rochester, NY 14627
Laboratory for Laser Energetics
Attn: Dr. R.S. Craxton
Dr. W. Seka

KMS Fusion
3941 Research Park Drive
P.O. Box 1567
Ann Arbor, MI 48106
Attn: Dr. F. Mayer

Institut fur Plasmaphysik
8046 Garching
Bei Munchen
West Germany
Attn: Dr. R. Sigel
Dr. H. Takabe c/o Dr. P. Mulser
National Research Council
Division of Physics
100 Susser Drive
Ottawa K1A-0R6, Canada
Attn: Dr. J. Alcock

University of Quebec
INRS Energie
Case Postale 1020
Varennes, Quebec
Attn: Dr. T. Johnston
Dr. R. Decoste

Rutherford Laboratory
Chilton, Didcot
Oxon OX110QX
England
Attn: Dr. M. Key
Dr. R. Evans

Sandia Laboratory
Albuquerque, NM
Attn: Dr. K. Matzen
Dr. J. Anthes
Dr. R. Palmer

Institute for Laser Engineering
Osaka University
Suita Osaka, 565
Japan
Attn: Dr. C. Yamanaka

Shanghai Institute of Optics and Fine Mechanics
Academia Sinica
Shanghai, PRC
Attn: Prof. Gan Fu-xi
Prof. Yu Wen-yan
Prof. Xu Zhi-zhan
Prof. Deng Xi-ming
Prof. Tan Wei-han
Mr. Pan Cheng-min

Soreq Nuclear Center
Yavne, Israel
Attn: Dr. A. Krumbein

INTERNAL DISTRIBUTION

Code 4040 J. Boris
J. Gardener
J. Orens

Sergio Morosi
Ist. Fisica Applicata
via Bassi 6 Pavia - ITALY

Defense Technical Information Center
Cameron Station
5010 Duke Street
Alexandria, VA 22314

Prof. G. Wallis
Prof. Klaus Junge
Zentralinstitut für Optik und Spektroskopie
DDR-1199 Berlin-Adlershof
Rudower Chaussee 6
West Germany

J. Balmer
Institute of Applied Physics
Sidlerstr. 5
CH-3012 BERN/Switzerland

Hn Qiguan
Lab. de Physique des Lasers
Uni. Paris Nord
93430 Villetaneuse/FRANCE

Gl. Barifi
Istituto Fisica Application
Universita di Paria
Pavia 27100 Italy

N.A. Tahir
Dept. of Nat. Phil
Glasgow University
Glasgow G12 (U.K.)

B. Meyer
HDE
CEL
BP27
94190 Villeneuve St. Georges
FRANCE

D. Unaugst
University of Jena
6900 Jena
Schlobgassel
Germ. Dem. Rep.

Patrick Flynn
Bldg. N73
Atomic Weapons Research Estab.
Aldermaston
Reading, U.K.

N. Kovalsky
Kurchatov Institute of Atomic Energy
D-182 Moscow USSR

J. Virmont
Ecole Polytechnique Gzeco ILM
Palaiseau 91127
FRANCE

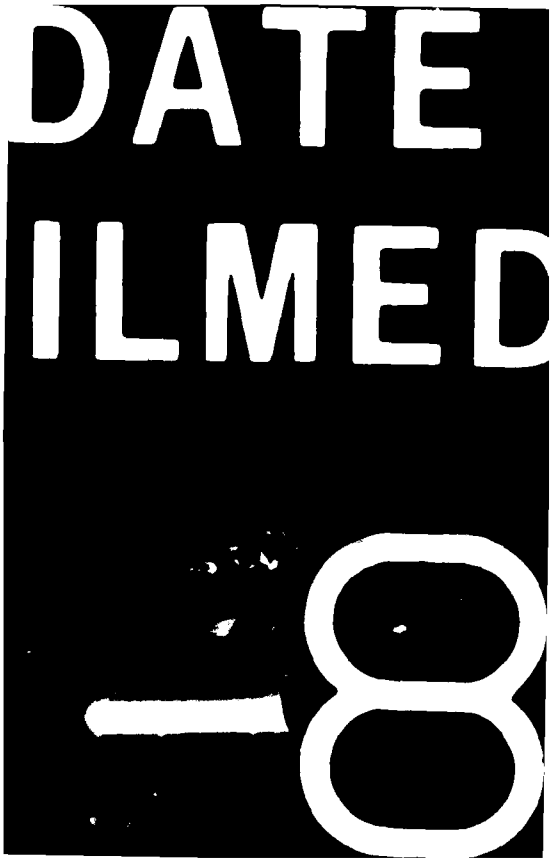
DATE
ILMED
8